

**Laboratoire M.S.M.A.P.** SARL

Microanalyse

Sciences des Matériaux Anciens et du Patrimoine - Etude des objets d'art

**STUDY OF A BRONZE VESSEL, *GU***

Assumed provenance and period: China, Shang dynasty



Detail view of the object.

---

*Analysis* : **Dr. B. DUBOSCQ**

Doctor of Quaternary geology  
and Prehistory  
Materials microanalysis Engineer.

**N. POIRIER**

Archaeometry engineer

## NOTICE

The purpose of this study, performed following established norms of scientific integrity, is to carry out scientific investigations to provide analytical data concerning the manufacturing mode of the studied cultural property, the possible weathering of its constitutive material, either natural or artificial and to characterize the deposits or surface treatments on the object.

The investigations based on optical examination and physicochemical analyses of samplings of the object; follow the methods briefly described in the report, which are long-standing standards and protocols employed by the scientific community.

Comparison of the results obtained with the data actually available in the scientific community allows concluding if the physical evidences of the object are consistent or not with its supposed origin and period of time.

These scientific investigations are carried out not taking into consideration historical research, iconography and stylistics statements about the object. Information about provenance, period or attribution of the cultural property are under the responsibility of the owner or its authorized agent and written in the report only as indication. However, this given information is used in the discussion for final statement.

M.S.M.A.P.

## OBJECTIVES

Study of a bronze vessel, *Gu* (H.: 32 cm, rim Ø: 17.5 cm, base Ø: 10 cm)  
Assumed provenance and period: China, Shang dynasty

Analysis of the manufacturing technique, the material from which the object is made, weathering, and any surface deposits, for determining whether it was subjected to natural, long-term weathering, compatible with its assumed age.

## SYSTEMS USED

Stereoscopic microscope, inverted optical metallographic microscope, scanning electron microscope (SEM) with back-scattered electron (BSE) and secondary electron (SE) imaging; coupled with energy-dispersive X-ray element analysis (EDX).

## SAMPLES

The study was performed by means of a sample of the base metal, taken from the base of the vessel (**P1**) and two replicas, one taken on a flaked part of the encrusting on the rim (**R1**) the other from the inscription area inside the base (**R2**).

Sample P1 was embedded in epoxy resin and a polished microsection perpendicular to its surface was performed. The microsection and the replicas were carbon coated for the SEM examination. This operation is partly responsible for the carbon (C) peak observed on the elementary X-ray spectra.

---

## STUDY RESULTS

This study examined the technique used to produce the object, the type of metal from which it was made, any weathering and visible surface deposits on top of the metal. Inspection and analyses revealed that:

- The object was made by casting a medium-tin (11%) low leaded bronze.
- There are evidences of the use of copper sulphide ores for the production of bronze. This characteristic is compatible with ancient metallurgy of bronze.
- The composition of this alloy, at our level of analysis accuracy, is consistent with those of ancient bronze vessels from China. No anomalies that could indicate the use of a "modern" bronze alloy were noted.
- The bronze of the vessel provides evidence that complex long-term corrosion has taken place:
  - deep leaching of the lead phases and replacement with cuprous oxide;
  - surface mineralization, selective corrosion of the  $\alpha$  and/or the  $\delta$  phase of the alloy, transgranular corrosion.
- Above the mineralised metal, several types of layered corrosion products are found: copper oxide, copper carbonate and lead carbonate, copper chloride.
- The corrosion occurred in a sedimentary environment, indicative of burying. This environment was biologically active, with high phosphorus and calcium suggesting a possible contact with calcium phosphate-rich material, bone for example.

**These characteristics are compatible with the object's assumed age.**

**1 - PRELIMINARY OBSERVATIONS**

The *Gu* has a complex patina, with areas where the metal appears “unaltered”, retaining the original yellow metallic and lustrous surface (Fig. 1a, M) and areas where the metal has a red to grey brown patina, covered with brightly-coloured red, blue and green corrosion products (Fig. 1a, arrows).

These corrosion products constitute crusting of variable thickness and granularity on top of the smooth metal surface (Fig. 1b, arrows).



Figure 1: Detail views of the object (a- middle part, b- upper part, c- inside of the vessel).

The corrosion seems to be more pronounced on the upper part of the *Gu*. The “unaltered” areas are located on the middle and bottom part of the vessel.

The metal surface shows slight chipping or scaling on protruding parts of the object, e.g. the rim or the base. The chipping and scaling reveal a bluish grey to purple coloured metal, with abundant cracks (Fig. 2a, arrows).

Fossil impressions of textiles of different types are observed outside the vessel on the upper part (Fig. 2b, arrows).

There are brownish-yellow earthy deposits preserved inside the vessel, and inside the base (Fig. 1c).

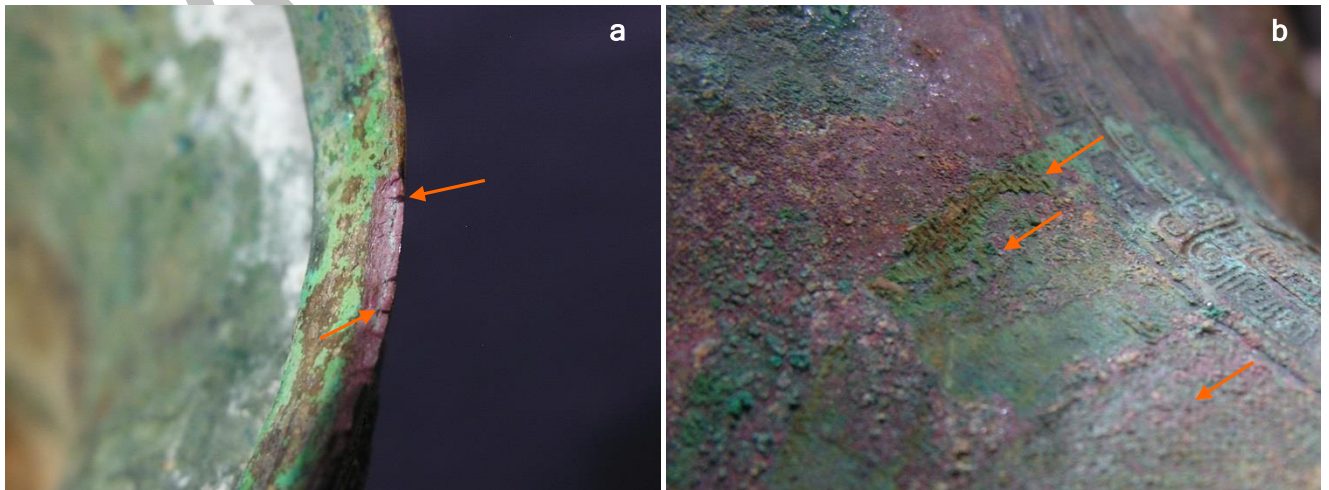


Figure 2: Detail views of the vessel (a- underside of the base rim, b- textile impression, upper part of the vessel).

## 2 - STUDY OF METAL AND OF CORROSION PROCESSES

### 2-1- The base metal

The metal sample was taken from the base (Fig. 3a, II), in area where the metal has a grey brown to bluish grey patina, under a red layer and red orange brown to green surface deposits.

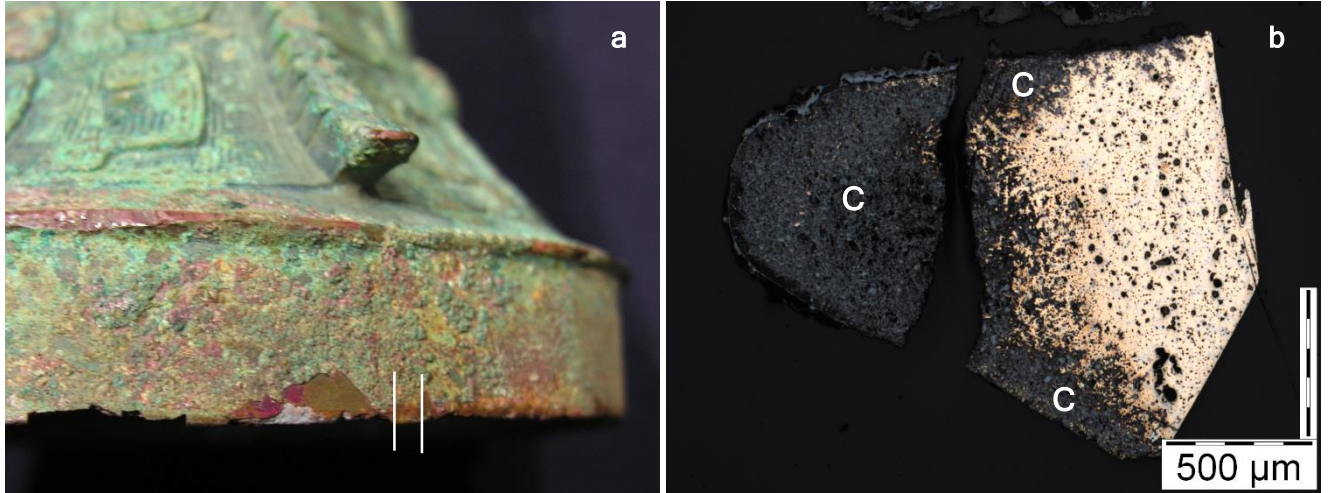


Figure 3: Localization of the metal sample (a-) and overall views of the microsection (inverted optical microscope, x 50, a- reflected light; b- polarized light). The square locates figure 4.

The microsection shows a dendritic microstructure (Fig. 3b), typical of casting process, with abundant interdendritic inclusions. The superficial corrosion layers (Fig. 3b, C) present a brown to red coloration (Fig. 3c, C).

Red orange to green deposits (Fig. 3c, orange arrows) cover the original metal surface.

Under polarized light, inclusions in the heart of the metal appear with a metallic aspect (Fig. 4a, orange arrows) and with a red coloration when they are localised in the corrosion layer (Fig. 4a, red arrows).

SEM-EDX analysis shows that these interdendritic inclusions are lead globules phases, appearing as white dots (Fig. 4b, orange arrows) in composition contest (BSE). The red inclusions in corroded areas are cuprous oxide replacing lead globules and appear as grey dots in SEM-BSE (Fig. 4b, red arrows).

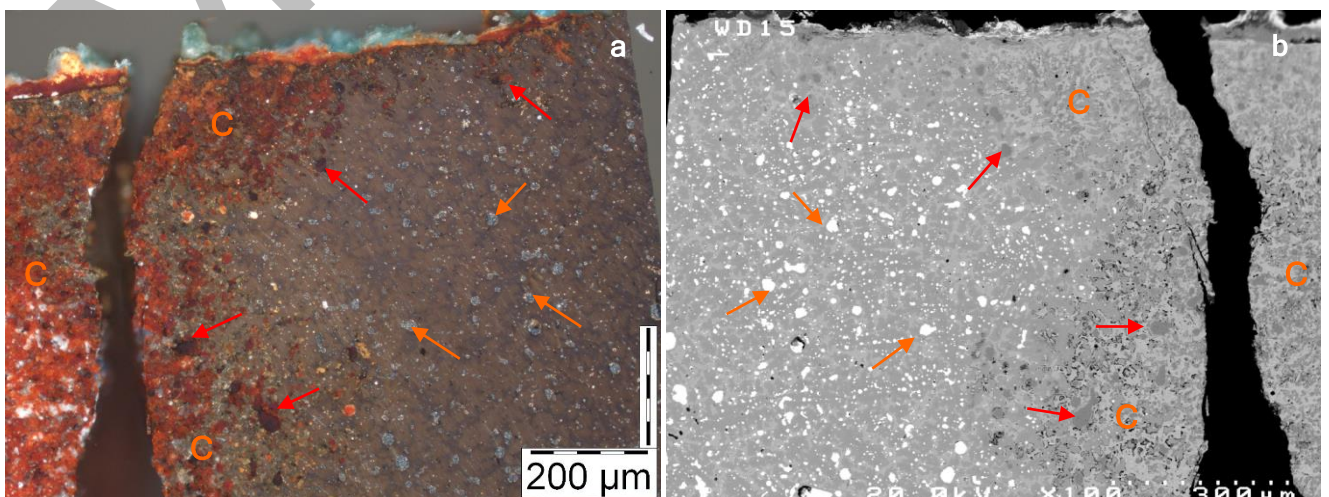
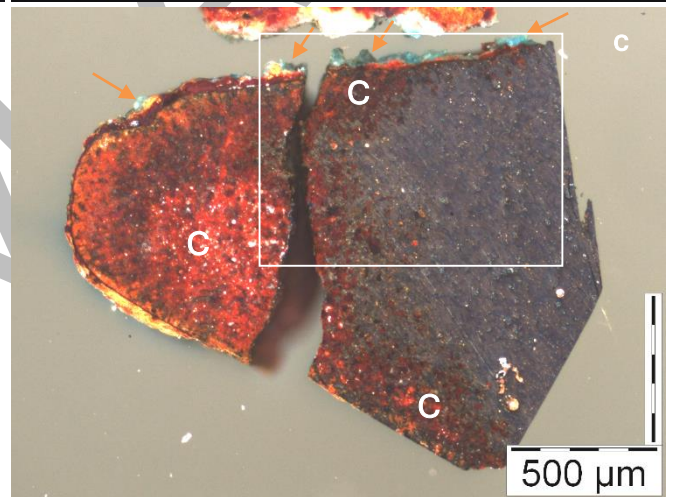


Figure 4: Detail views of the microsection, (same field, x 100, a- inverted optical microscope, b- SEM, BSE).

## 2-2- Analysis of the metal

Semi-quantitative analysis of the base metal of the vessel was carried out, from three areas of metal where metallic lead globules were preserved. The results are listed in the table 1 below (% of each element):

The experimental conditions were as follows: accelerating voltage  $V=30\text{KV}$ , acquisition time  $T=50$  seconds, working distance  $WD=15$  mm, area examined  $\times 100$ . The results obtained are expressed as an elemental atomic percentage [also known as percentage composition] normalised to 100%.

For EDX analysis, the detection threshold is deemed to be of the order of 1000ppm and measurement accuracy is of the order of 1% for the major elements under optimum conditions.

Elements that were not detected and those of which the levels detected were less than or equal to the uncertainty of measurement have been flagged using the abbreviation "nd" (for "not detected"). For such elements, when the levels measured are less than 1%, the fact that a value is listed is first and foremost an indication that the element is actually present in the sample in question.

Cu	Sn	Pb	Fe
83.4	11.0	4.4	1.1
85.2	10.0	4.2	0.7
84.8	9.8	4.7	0.7

The metal used to cast the *Gu* is bronze, with medium tin content (10 to 11%) and low lead content (4 to 5%). Traces of iron (1%) are detected.

The tin level of bronze leads to a segregation phenomenon of intermetallic phases including a hard, silver-white, richer in tin (Fig. 5a,  $\delta$  and 5b), which gives the metal a light colour, whereas the other  $\alpha$  phase (Fig. 5a,  $\alpha$ ) with a higher copper content has a golden colour.

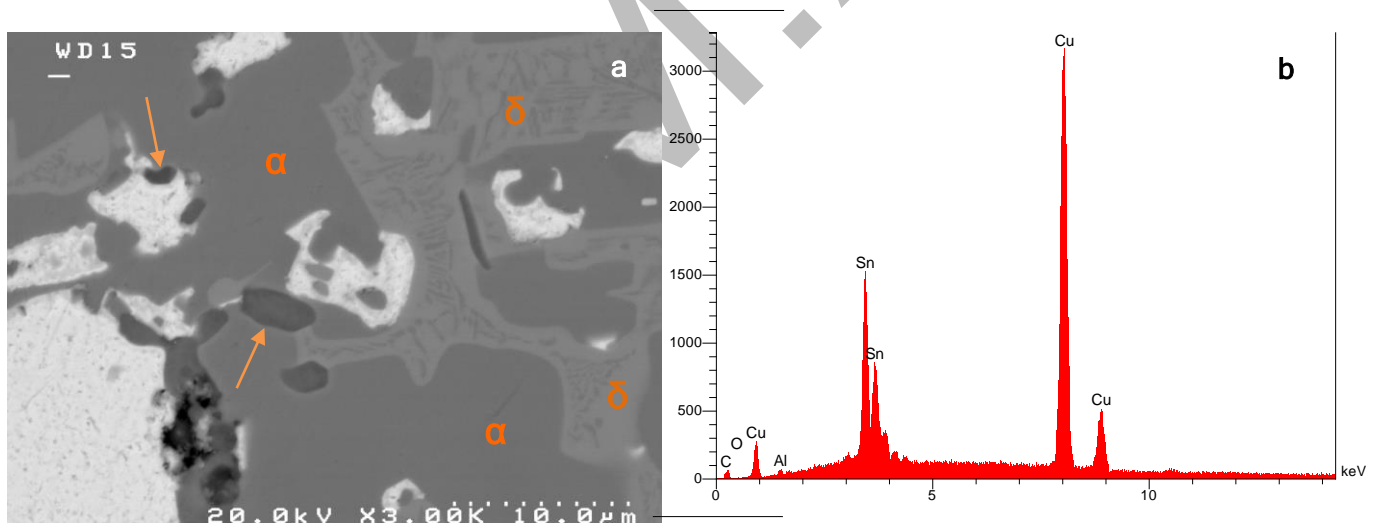


Figure 5: Detail view of the metal microstructure (a- SEM, BSE,  $\times 3000$ ) and EDX analysis spectra of the rich-tin phase (b-) and iron-copper sulphide inclusion (c-).

$\delta$  compound generally has a characteristic eutectoid microstructure (Fig. 5a,  $\delta$ ) and is very closely linked to  $\alpha$  phase and lead phases.

Traces of iron detected correspond to non-metallic iron-copper sulphide inclusions present in the bronze (Fig. 5a, arrows and Fig. 5c), in close relationship with the lead phases.

*Iron is one of the main impurities detected in ancient bronze pieces from China (see bibliography, ref. 1).*

*The presence of iron-copper sulphide inclusions in the alloy indicates the use of copper sulphide ores for the production of bronze. This characteristic is compatible with ancient Chinese metallurgy of bronze.*

The composition of this alloy, at our level of analysis accuracy, is consistent with those of ancient bronze vessels from China. No composition anomalies that could indicate the use of a “modern” alloy were noted.

### 2-3- Corrosion processes

The sample provides evidence that the material was weathered in different stages, a process which resulted in areas with distinct appearances and compositions (Fig. 6, **C1**, **C2**, **C3**, **C4**), above the sound base metal (Fig. 6a, **M**), characterised by the preservation of metallic lead globules.

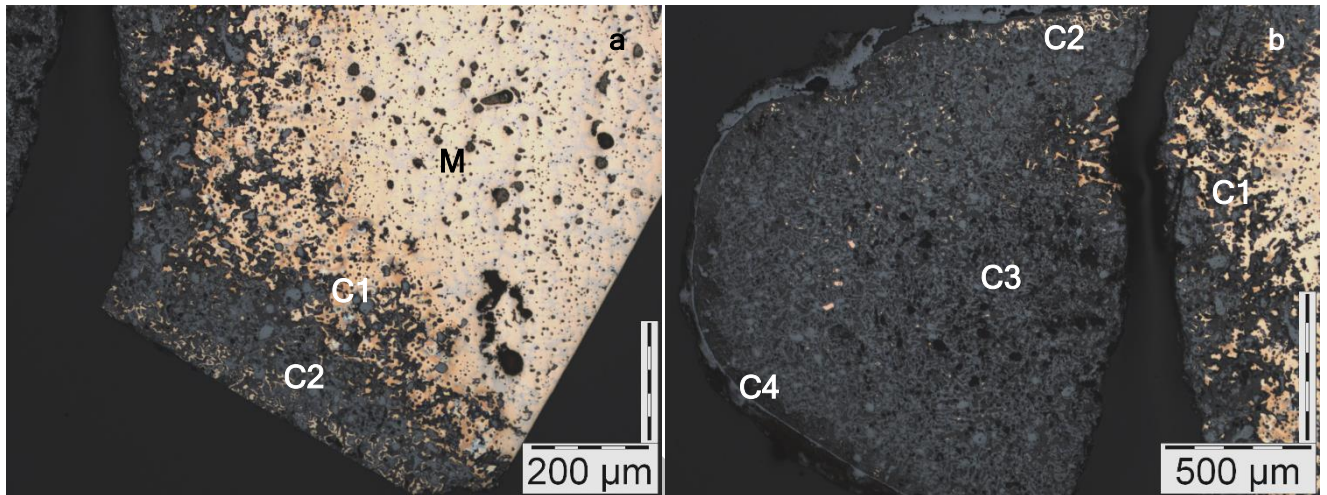


Figure 6: Detail views of the microsection (inverted optical microscope, a- x 100, b- x 50).

We carried out semi-quantitative analysis of the different areas. The results are listed in the table 2 below (% of each element):

Areas/Elements	Cu	Sn	Pb	Fe	As	Cl	Al
<b>M (base metal)</b>	83.4	11.0	4.4	1.1	nd	nd	nd
<b>C1</b>	73.4	14.4	5.0	1.0	2.8	2.2	1.4
<b>C2</b>	65.2	18.6	7.0	1.1	3.1	4.4	0.7
<b>C3</b>	62.4	19.4	8.1	1.5	4.7	4.7	1.0
<b>C4</b>	58.8	21.0	8.9	1.5	4.9	5.0	nd

Generally, corrosion is evidenced by a relative increase in tin and lead close to the metal's surface.

This is due to the copper migrating to the outside where it has formed the surface deposits ranging in colours from orange red to green blue (Fig. 3c, orange arrows).

In the corroded areas, there is a perceptible amount and enrichment of chlorine, and traces of aluminium. These elements are likely to have come from the environment in which the vase was buried.

The iron content is approximately the same. We will discuss later the presence of arsenic in the corroded areas.

The different areas observed correspond to several types of corrosion:

**The base metal:**

In the areas where the base metal is not affected by corrosion processes, the  $\delta$  and  $\alpha$  phases do not appear altered and lead globules still present their original metallic aspect.

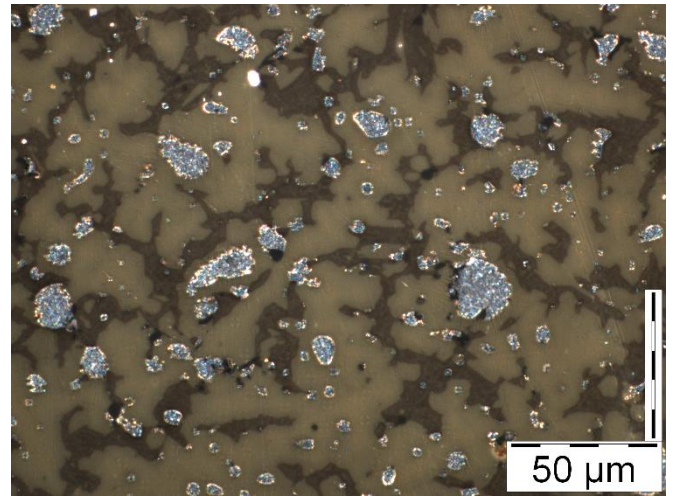


Figure 7: Detail view of the microsection (inverted optical microscope, polarized light, x 500).

**Area C1:**

In this area, corrosion affects the lead phases in interdendritic location (Fig. 8a, arrows). The metallic lead has here been replaced by lead salts, then red copper oxide (Fig. 8b) has in turn replaced the corroded lead phases.

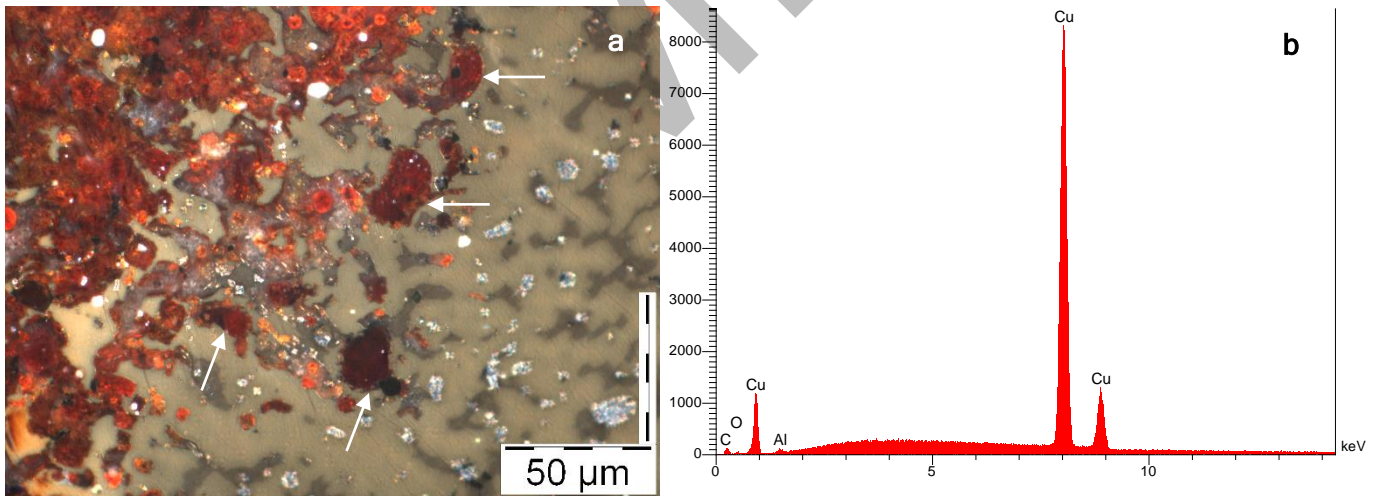


Figure 8: Detail view of the microsection in corrosion area C1 (a-, inverted optical microscope, polarized light, x 500) and EDX analysis spectrum (b-) of a lead phase affected by alteration with copper oxide replacement.

*The leaching of lead and its replacement by copper oxide is a phenomenon that is typically associated with ancient bronze from China (ref. 1).*

At the same time, complete selective corrosion of  $\delta$  phase (Fig. 9,  $\delta$ ) is observed. The first signs of alteration of  $\alpha$  compound (Fig. 9,  $\alpha$ ) are visible on the surround of the phase (Fig. 9b, arrows).

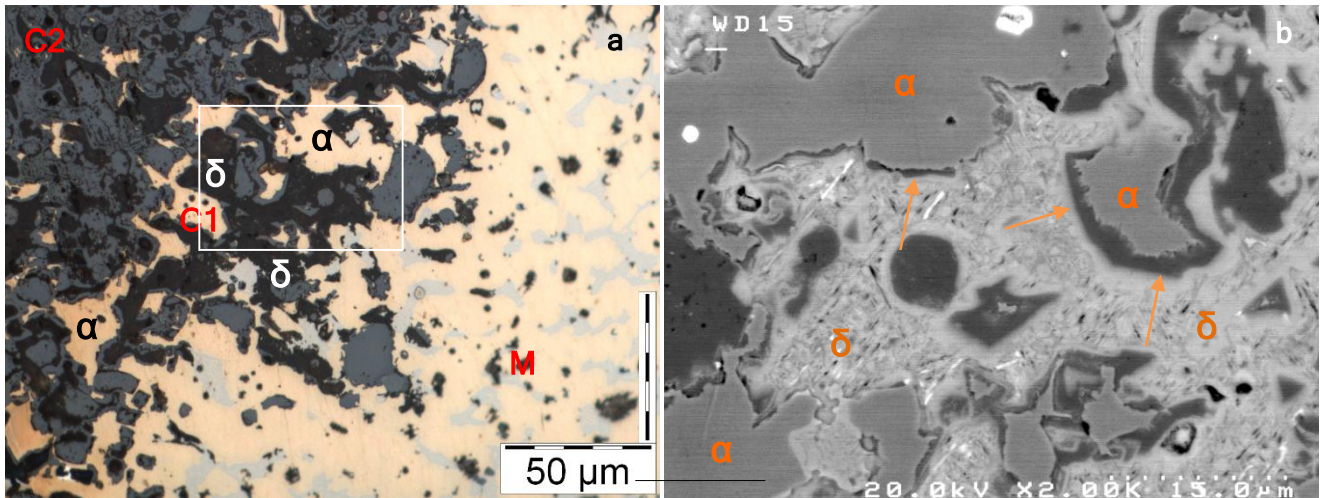
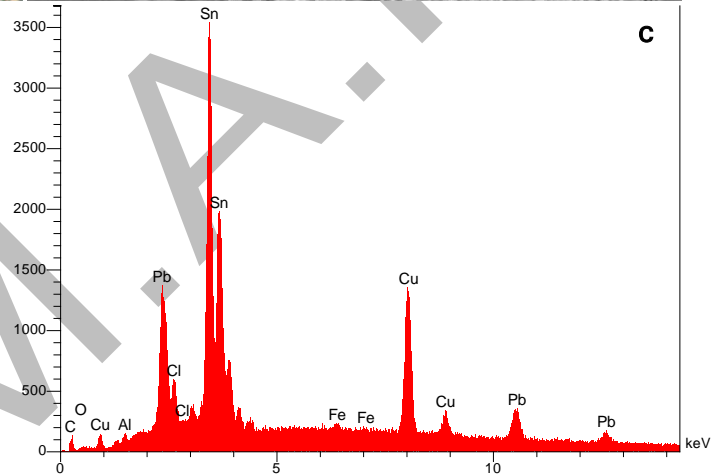


Figure 9: Detail views of the microsection in corrosion area C1 (a-, inverted optical microscope, x 500, b-, SEM, BSE, x 2000) and EDX analysis spectrum (c-) of the corroded  $\delta$  phase. The square locates figure 9b.

From a chemical point of view there is an increase in tin and lead content and a decrease in copper (Table 2). Some arsenic, chlorine and aluminium are detected.



**Area C2:**

In this area (Fig. 10) the corrosion process has increased. All  $\alpha$  and  $\delta$  phases are corroded. However, in some place, superficially and under the corrosion products deposits (Fig. 10, D) some of the  $\alpha$  phase is not altered.

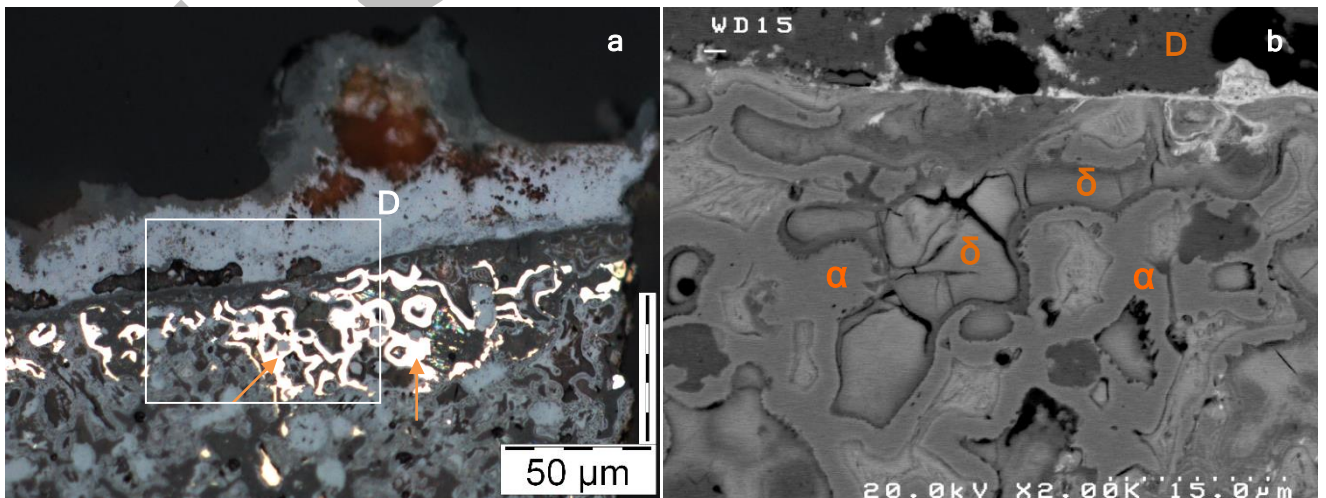


Figure 10: Detail views of the microsection in corrosion area C2 (a-, inverted optical microscope, x 500, b-, SEM, BSE, x 2000). The square locates figure 10b.

From a chemical point of view there is an increase in tin and lead content and a decrease in copper (Table 2). Arsenic and chlorine are also more abundant.

**Area C3:**

This area appears almost completely mineralized by corrosion of  $\alpha$  and  $\delta$  compounds (Fig. 11). Only few remains of  $\alpha$  phase are visible (Fig. 11b, arrows).

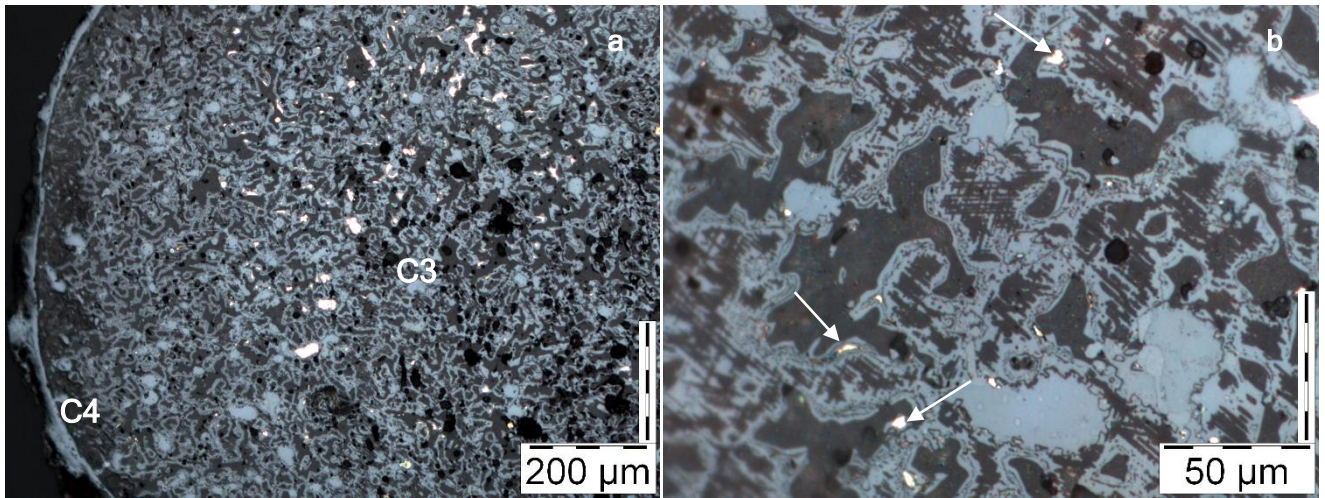


Figure 11: Detail views of the microsection (a-, inverted optical microscope, x 100) and of the corrosion in area C3 (b-, inverted optical microscope, x 500).

Area C3 presents the same chemical evolution as previously observed in areas C1 and C2, with particularly an increase in tin and lead content (Table 2).

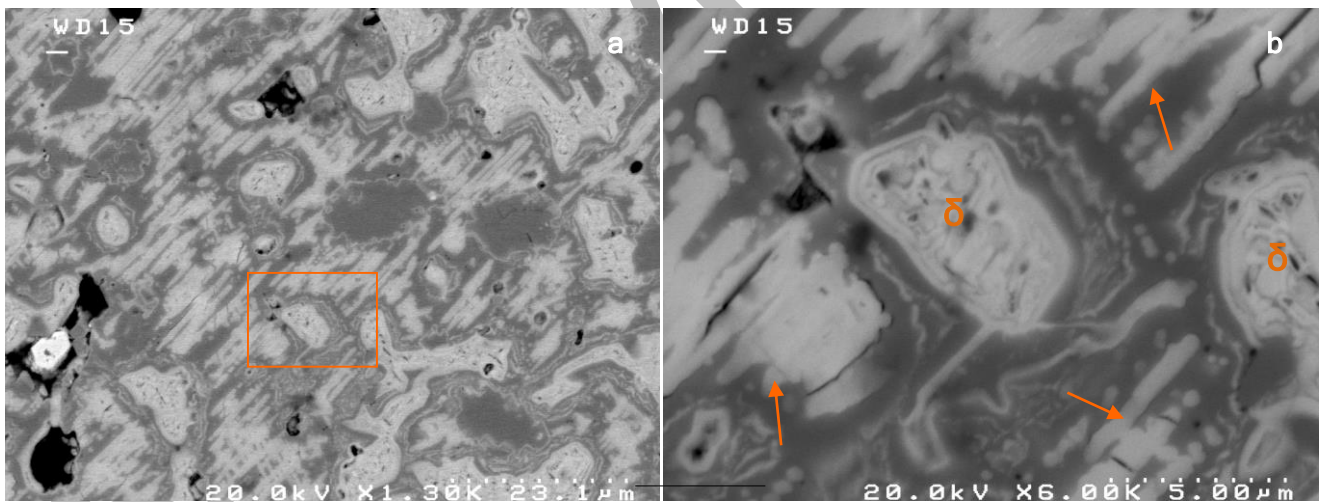
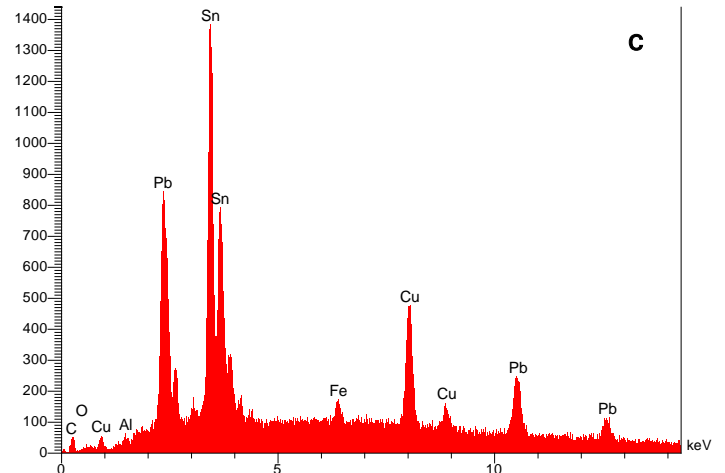


Figure 12: Detail views (SEM, BSE, a- x 1300, b- x 6000) and EDX analysis spectrum (c-) of the transgranular corrosion. The square locates figure 12b.

Transgranular corrosion affects the  $\alpha$  phase (Fig. 12a, 12b, arrows) and results in high tin and lead compounds (Fig. 12c).

This localized phenomenon is the result of mechanic stress in this area which is localised on the edge of the vessel.



**Area C4:**

This area is completely mineralized (Fig. 13), with the highest tin levels (Table 2).

*Surface mineralization is characteristic (ref. 2) of the weathering of bronze with high levels of tin. It allows the preservation of the original metal surface and develops a characteristic smooth and shining greyish patina as observed on the Gu under surface encrusting.*

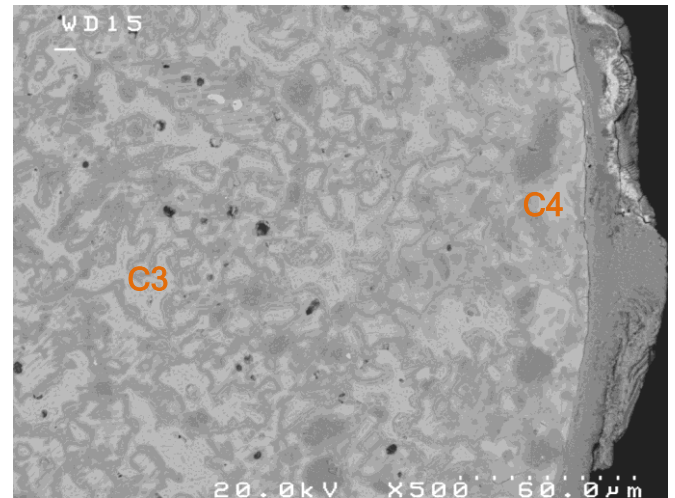


Figure 13: Detail view (SEM, BSE, x 500) of the microsection in corrosion areas C3 and C4.

**The corrosion phenomena that have affected this object are complex. They relate directly to the level of tin in the alloy (selective corrosion of phase  $\delta$ , superficial mineralized layer) and to the presence of lead. They are the result of long-term changes.**

The systematic detection of arsenic in the corroded areas is notable, as this element was not detected in the base metal. Its appearance is obviously in relationship with the corrosion processes. Several hypotheses can be proposed:

- arsenic is present in the base metal, but under the detection limit. The corrosion processes lead to an increase in the concentration, as tin for example.  
*In the corroded areas, arsenic is detected in lead-rich structures. It is possible that arsenic is present in the base metal in lead globules.*
- arsenic comes from the environment, but no arsenic is detected in the sedimentary deposits on the object.
- arsenic is the result of a surface treatment.

*If no clear evidence of such treatment has been observed in Chinese metallurgy the presence of arsenic in some ancient Chinese bronze vessel and mirror patina has been previously detected (ref. 3).*

### 3 - STUDY OF SURFACE DEPOSITS

#### 3- 1- Deposits on the microsection

Different surface deposits overlay the superficial corroded layer (Fig. 14a, C2): red layer (Fig. 14, 1) in direct contact with the original metal surface and superposition of orange (Fig. 14, 2), white (Fig. 14, 3) and blue green (Fig. 14, 4) layers.

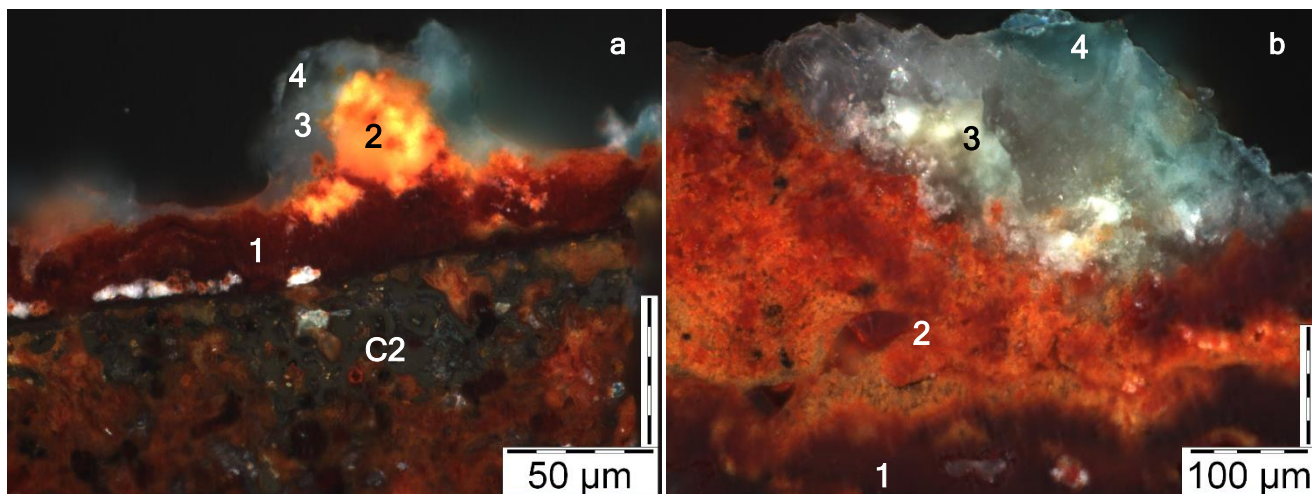


Figure 14: Overall views (inverted optical microscope, polarized light, a- x 500, b- x 200) of the deposits surface.

**The red layer** (Fig. 14 and 15a, 1) consists of finely crystallized copper oxide with some lead-rich areas (Fig. 15a, arrows).

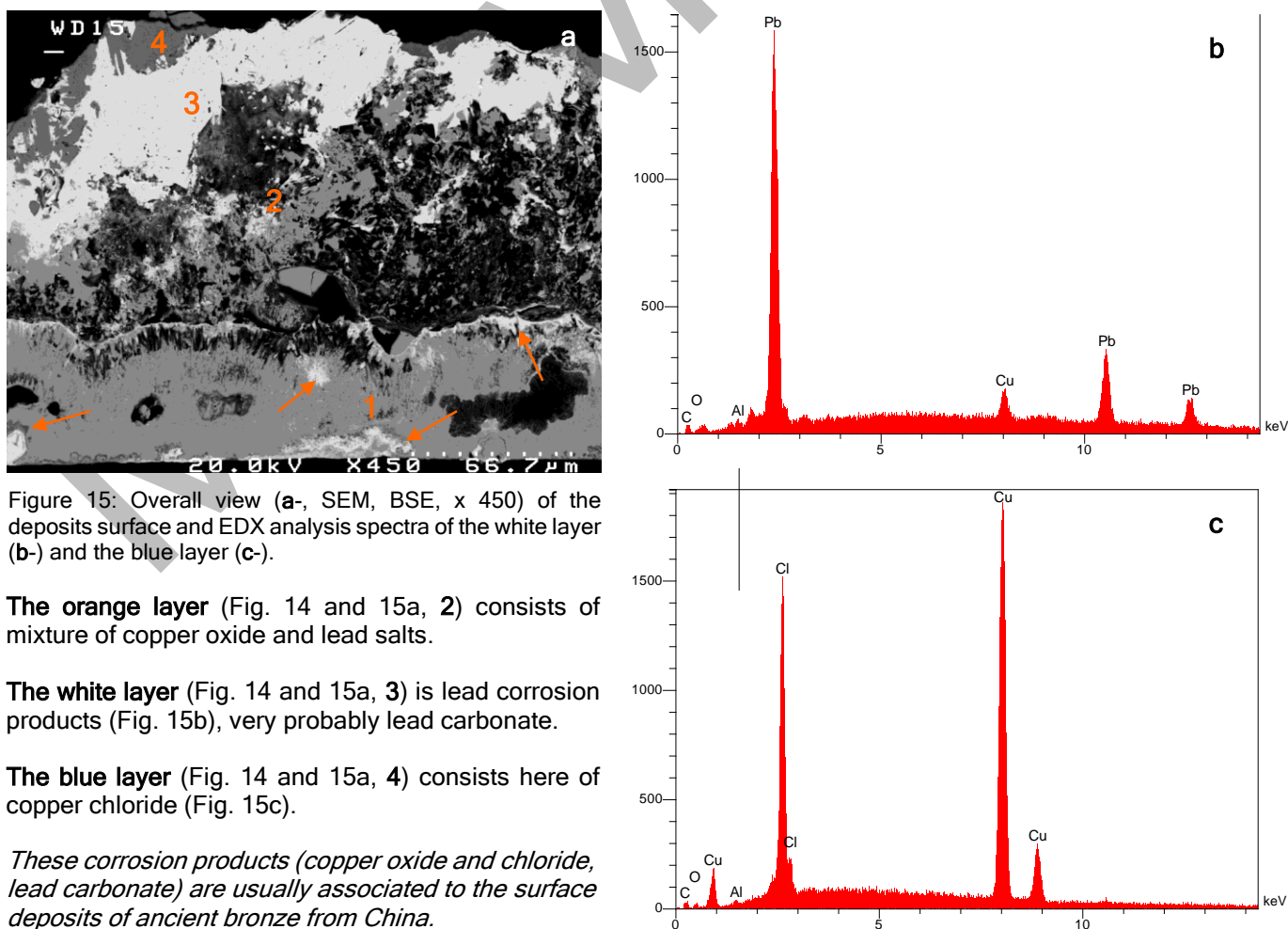


Figure 15: Overall view (a-, SEM, BSE, x 450) of the deposits surface and EDX analysis spectra of the white layer (b-) and the blue layer (c-).

**The orange layer** (Fig. 14 and 15a, 2) consists of mixture of copper oxide and lead salts.

**The white layer** (Fig. 14 and 15a, 3) is lead corrosion products (Fig. 15b), very probably lead carbonate.

**The blue layer** (Fig. 14 and 15a, 4) consists here of copper chloride (Fig. 15c).

*These corrosion products (copper oxide and chloride, lead carbonate) are usually associated to the surface deposits of ancient bronze from China.*

### 3- 2- Deposits on the replicas

#### Replica R1



Replica R1 was taken on the outside of the rim, in an area of patina scaling off.

The replica detached the brittle crusting, with red orange areas (Fig. 16, Fig. 19a, R), shining grey (Fig. 16, Fig. 19a, G) and blue-green to grey-green (Fig. 16, Fig. 19a, GG) areas, overlaid with bright green to yellowish-green products (Fig. 16, arrows).

Figure 16: Detail view (stereoscopic microscope, x 5) of the deposits on replica R1.

The red orange crusting consists mainly of finely crystallized copper corrosion products (Fig. 17a, Cu), with some lead-rich corrosion products areas (Fig. 17a, Pb) as observed in the base layer of the crusting in sample P1 (cf. Fig. 15a).

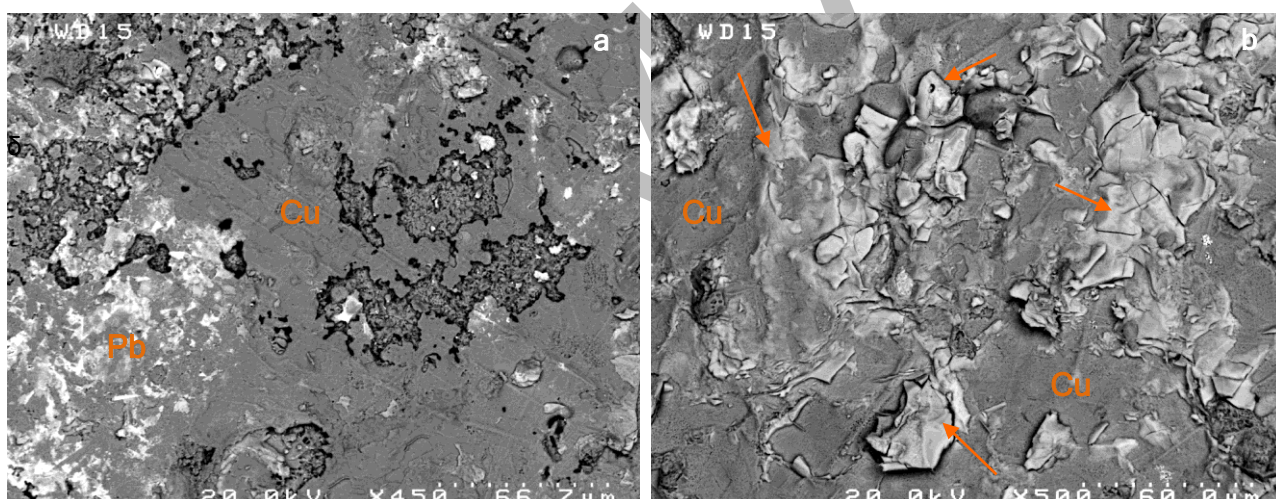
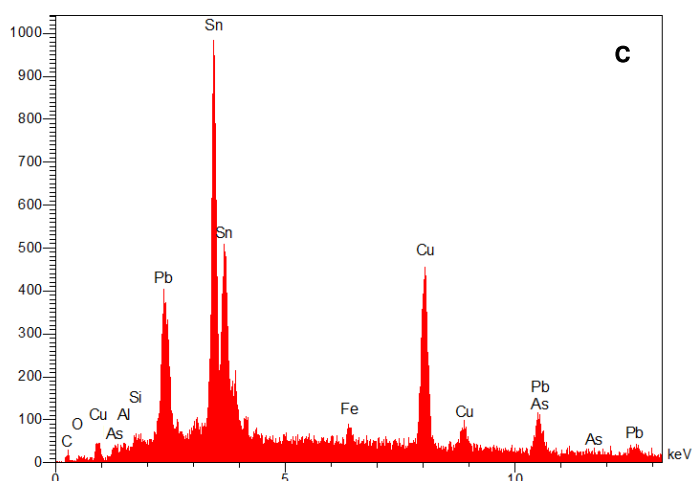


Figure 17: Detail views (SEM, BSE, a- x 450, b- x 500) of the flaked-off crusting in replica R1 and EDX analysis spectrum (c-) of the shining grey crusting.

The shining grey areas in the crusting show copper-tin and lead-rich phases (Fig. 17b, arrows), in a copper-rich matrix (Fig. 17b, Cu), which are similar in composition (Fig. 17c) and morphology to the corroded area C3 in sample P1 (cf. Fig.12).



The grey-green areas are high-tin compounds which clearly show the  $\delta$  phase eutectoid structure (Fig. 18,  $\delta$ ), with porosities left by lead globule leaching (Fig. 18, arrows).

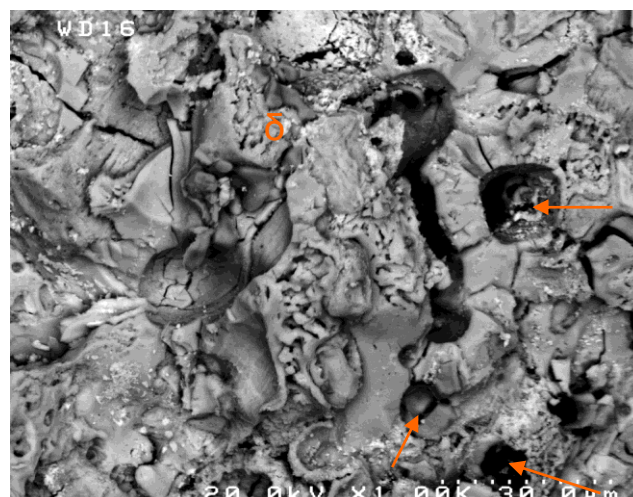


Figure 18: Detail view (SEM, BSE, x 1000) of the grey-green crusting area. Replica R1.

The grey and grey-green areas on the crusting correspond to mineralized and corroded metal superficial layer as observed in sample P1 section.

*The corrosion phenomena and surface crusting in the upper part of the vessel are similar to what is observed in the lower part.*

The bright green to yellowish-green products (Fig. 19a, arrows) are in direct contact with the red orange crusting (Fig. 19a, R).

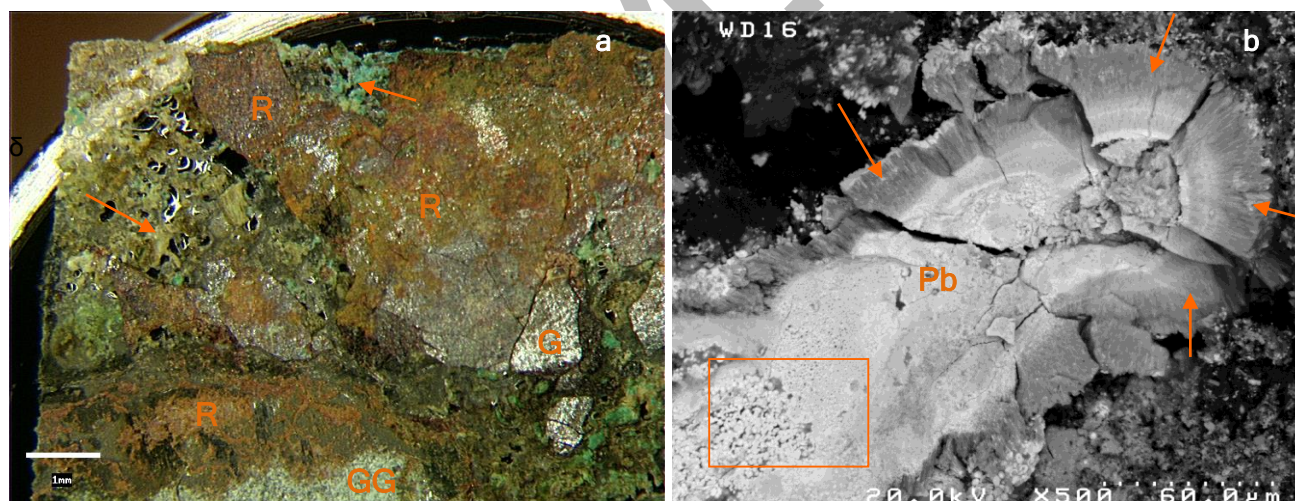
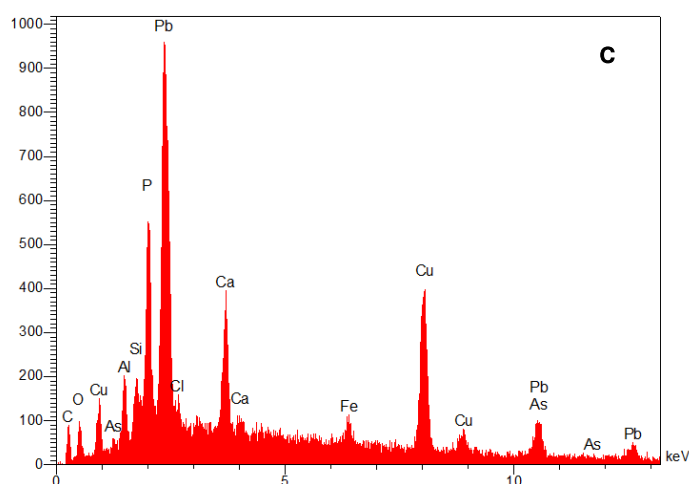


Figure 19: Detail views (a- stereoscopic microscope, x 14, b- SEM, BSE, x 500) and EDX analysis spectrum (c-) of the bright-green deposits on replica R1. The square locates Fig. 20b.

They consist in finely crystallized fibrous material (Fig. 19b, arrows) where, besides lead and copper, phosphorus, calcium, silicon, aluminium and iron are detected, with traces of arsenic (Fig. 19c).



In contact with the crusting (Fig. 19a, Pb), phosphorus and lead-rich area (Fig. 20a) show a specific hollow micro spherical morphology (Fig. 20b, arrows) which can be related to microbial presence (very probably bacteria).

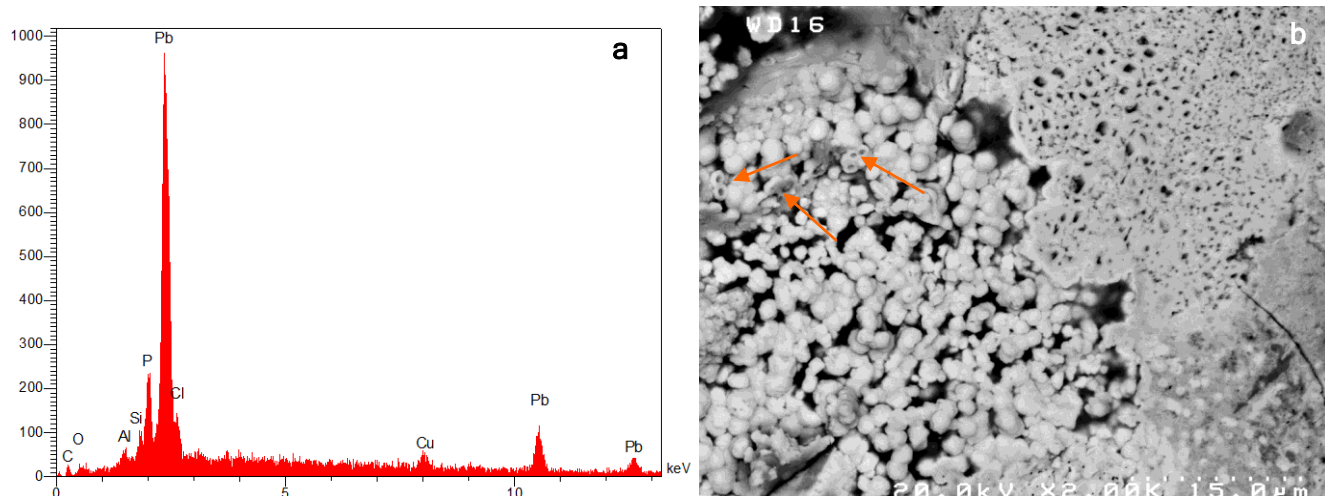


Figure 20: EDX analysis spectrum (a-) and detail view (b-, SEM, BSE, x 2000) of the lead-rich area in the bright-green products. Replica R1.

*Phosphorus is often detected at several percent levels in bronze vessels patina, together with silicon, aluminium and iron (ref. 4). These elements come from the burying environment of the object.*

*The presence of bacterial remains, associated with high calcium suggests a possible contact with calcium phosphate-rich material, bone for example.*

**These different characteristics: deep leaching of the lead phases and replacement by copper oxides, selective corrosion of the  $\alpha$  and/or the  $\delta$  phase of the alloy, superficial mineralization of the metal, transgranular corrosion, diversity of the surface corrosion products, indicate that the object was subjected to long-term weathering compatible with its assumed age, in a buried sedimentary biologically active and phosphorus-rich environment.**

#### 4 - STUDY OF THE INSCRIPTION AREA

##### Replica R2

The inscription area is characterized by yellowish-green to brownish deposits, which are present as well in the bottom of the inscription (Fig. 21b, orange arrows), the vertical sides (Fig. 21b, white arrow) and the vessel surface (Fig. 21b, blue arrows).

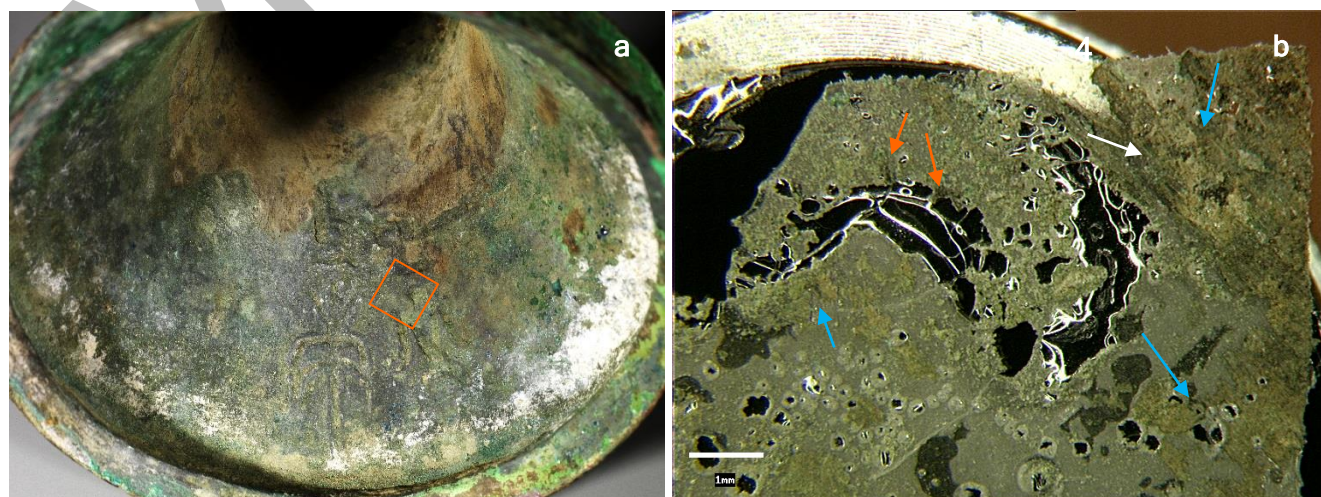


Figure 21: Overall view of the inscription (a-) and detail view (b-, stereoscopic microscope, x 14) of replica R2.

These products are phosphorus and calcium-rich corrosion products of copper, lead and tin, with silicon aluminium, and iron (Fig. 22a). Arsenic traces are detected.

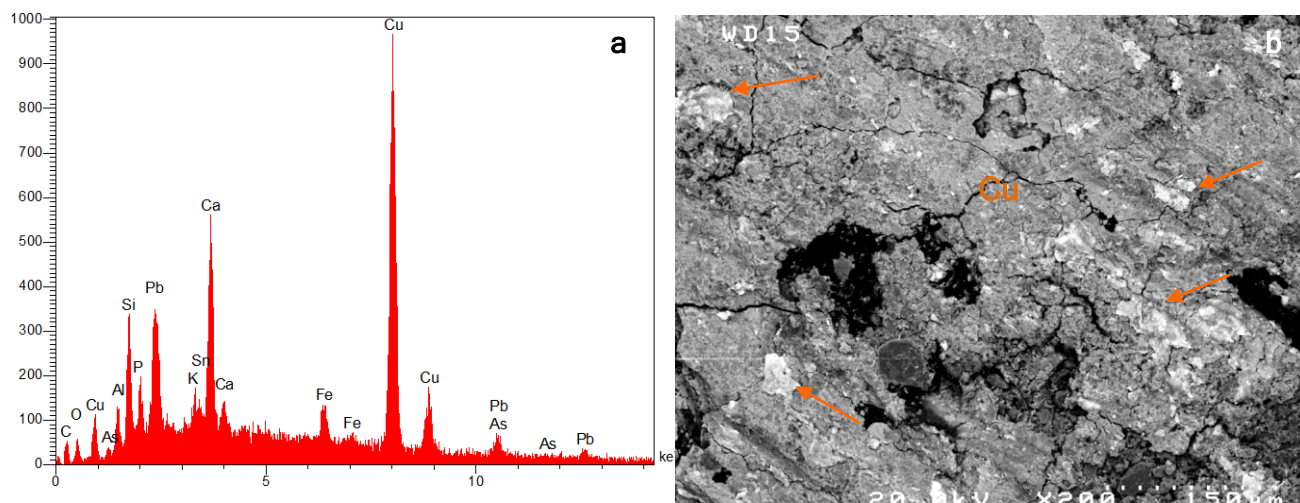


Figure 22: EDX analysis spectrum (a-) and detail view (b- SEM, BSE, x 200) of the surface deposits in the inscription area. Replica R2.

The copper high matrix (Fig. 22b, Cu) contains lead or tin-rich areas (Fig. 22b, arrows).

**The presence of the same type of deposit covering the inscription and the vessel surface in the inside of the base, as in the upper part of the vessel is indicative of the authenticity of the inscription.**

## Bibliography

- (1) - R.J. GETTENS, 1969, The Freer Chinese Bronzes, Vol. II, *Technical Studies, Oriental Studies*, N°7, Smithsonian Institution, Freer Gallery of Art, Washington.
- (2) - N. MEEKS, 1993, Patination phenomena on Roman and Chinese high-tin bronze mirrors and other artefacts. *Metal plating and Patination*, Butterworth-Heinemann Ltd. pp. 61-84.
- (3) - P. COLOMBAN, A. TOURNIE, M. MAUCUER, p. MEYNARD, 2012, On-site Raman and XRF analysis of Japanese/Chinese bronze/brass patina - the search for specific Raman signatures., *Journal of Raman spectroscopy*, 2012, 43, pp. 799-808.
- (4) - Z. SHOUKANG, H. TANGKUN, Studies of ancient Chinese mirrors and other bronze artefacts. *Metal plating and Patination*, Butterworth-Heinemann Ltd. pp. 50-62.